$SrTiO_3$ Displacive Transition Revisited via Coherent X-Ray Diffraction

S. Ravy,[1] D. Le Bolloc'h,[2] R. Currat,[3] A. Fluerasu,[4] C. Mocuta,[4] and B. Dkhil[5]

[1]*Synchrotron SOLEIL, L'Orme des merisiers, Saint-Aubin BP 48, 91192 Gif-sur-Yvette cedex, France*
[2]*Laboratoire de physique des solides, Université Paris-sud, CNRS, UMR 8502, F-91405 Orsay Cedex, France*
[3]*Institut Laue-Langevin, 6, rue Jules Horowitz, Boîte postale 156, 38042 Grenoble Cedex 9, France*
[4]*European Synchrotron Radiation Facility, 6 rue Jules Horowitz, Boîte postale 220, 38043 Grenoble Cedex, France*
[5]*Laboratoire Structures, Propriétés et Modélisation des Solides, Ecole Centrale Paris, CNRS, UMR 8580, Grande Voie des Vignes, F-92295 Chatenay-Malabry Cedex, France*

(Received 10 November 2006; published 5 March 2007)

We present a coherent x-ray diffraction study of the antiferrodistortive displacive transition of $SrTiO_3$, a prototypical example of a phase transition for which the critical fluctuations exhibit two length scales and two time scales. From the microbeam x-ray coherent diffraction patterns, we show that the broad (short-length scale) and the narrow (long-length scale) components can be spatially disentangled, due to 100-μm-scale spatial variations of the latter. Moreover, both components exhibit a speckle pattern, which is static on a $\sim$10 mn time scale. This gives evidence that the narrow component corresponds to static ordered domains. We interpret the speckles in the broad component as due to a very slow dynamical process, corresponding to the well-known *central* peak seen in inelastic neutron scattering.

DOI: 10.1103/PhysRevLett.98.105501 PACS numbers: 61.10.−i, 68.35.Rh, 77.84.Dy

Although most issues concerning the application of scaling theory to structural phase transitions have been settled long ago (see, e.g., [1]), two frequently observed scattering features remain unaccounted for within standard scaling theory: the ''neutron'' central peak (CP) and the ''x-ray'' narrow component (NC). Remarkably, both features were first evidenced in studies of the critical behavior associated with the $T_c = 100$–105 K antiferrodistortive transition in the perovskite $SrTiO_3$.

The first issue concerns the time scale of the critical fluctuations. While far above T_c, the fluctuations time scale is governed by the inverse soft-phonon frequency, a few degrees above T_c a narrow *central* (i.e., zero-frequency) line appears in the inelastic neutron scattering data [2,3], whose weight grows critically on approaching T_c. Its frequency width $\Delta\nu$ is too small to be resolved by neutron techniques [4], but EPR measurements [5] have set an upper bound of $\Delta\nu < 0.6$ MHz. There is substantial evidence [6,7] that the CP phenomenon is connected with slowly relaxing or frozen bulk defects, such as vacancies or interstitials, but direct measurements of the relaxation time associated with these defects is still missing.

Beside this second *time scale*, another unresolved issue concerns the occurrence of a second *length scale* in the critical fluctuations. As previously mentioned, the structural phase transition in $SrTiO_3$ has been the first example [8] where a narrow Lorentzian-squared ($\mathcal{L}^2$) component in the critical x-ray scattering profiles has been observed close to T_c, in addition to the usual and broader Lorentzian ($\mathcal{L}$) component (BC). It is now well established by high resolution x-ray diffraction techniques that critical fluctuations close to structural and magnetic phase transitions involve two distinct pretransitional scattering components [9], each one corresponding to a diverging length scale, as T approaches T_c.

Furthermore, it has been shown at least in Ho [10] and $SrTiO_3$ [11,12] that the NC is sample dependent, and that its critical behavior is different from that of the BC, with larger critical exponents. The NC component was found to depend on surface preparation [12,13], and to arise from a near surface *skin* region (typically 10 to 100 μm thick). This reinforced the conclusion that the NC was somehow connected with surface disorder and many studies concluded that long-range strains localized near the surface were responsible for the occurrence of the NC [11,12,14].

Because of the similarities in the two phenomena, the question arose as to whether the neutron CP was related to the x-ray NC [15]. From a neutron reinvestigation of the critical scattering of $SrTiO_3$, it was shown that both phonon softening and CP were needed to account for the x-ray BC [16]. From this result and the absence of NC in the neutron high resolution study, it was concluded that the CP was in fact not correlated with the NC [16]. In both phenomena, however, it is striking that the time scale was never experimentally obtained, first because the NC is absent from the neutron data, and second because the CP energy width is not resolved. This is the reason why we have performed coherent x-ray diffraction (CXD) on the critical scattering of $SrTiO_3$.

With the advent of third generation synchrotron light sources, it has become possible to perform x-ray diffraction with a coherent beam [17], a technique which has since proved to be a powerful tool to probe disordered systems. Indeed, CXD no longer results in smooth ensemble-averaged diffraction patterns but in speckled patterns, which are related to the exact distribution of scatterers within the radiation's coherence volume. Moreover, the temporal evolution of the speckles allows one to access the dynamics of the system, especially in the 1–10^4 s range (see, e.g., [18]). In this Letter, we show how

CXD experiments performed on $SrTiO_3$ in the vicinity of its antiferrodistortive phase transition have succeeded in shedding a new light on the CP and NC issues.

Preliminary experiments have been performed at the ID10a and the ID01 beam lines of the ESRF. The results presented here were obtained at ID10a, using a Si(111) single-crystal monochromator to get 8 keV x rays. A $SrTiO_3$ single crystal, grown by the top-seeded technique, with a 4 mm $\times$ 4 mm polished [110] face, was mounted in a top-loading cryostat and aligned with the (311) and (1, $\bar{1}$, $\bar{2}$) directions in the horizontal scattering plane. The geometry of diffraction to reach the $\mathbf{Q}_s = (\frac{3}{2}, \frac{1}{2}, \frac{1}{2})$ superstructure reflection (Bragg angle $\theta_B = 19.2°$, $Q_s = 2.68$ Å^{-1}) was thus strongly asymmetric with the incident angle $\theta_i = 13°$ and the exit angle $\theta_f = 25.4°$. Given the $\mu^{-1} \sim 17$ μm penetration length of 8 keV x rays, this leads to an effective penetration of 3.8 μm.

The conditions to get a coherent beam were obtained by using 10 μm $\times$ 10 μm entrance slits (playing the role of pinhole) 20 cm before the sample. The beam quality and its intrinsic degree of coherence were tested by using 2 μm $\times$ 2 μm entrance slits [19], in order to observe their regular interference fringes in the Fraunhofer regime. Guard slits have been placed after the entrance slits to reduce parasitic slit scattering. The patterns were recorded on a direct illumination CCD camera (20 μm $\times$ 20 μm pixel size) located 1.8 m after the sample, yielding a resolution of 4.5×10^{-5} Å^{-1} per pixel.

We first checked the phase transition characteristics by measuring the scattering around the $\mathbf{Q}_s$ superstructure reflection as a function of temperature, using a point detector and 20 μm $\times$ 20 μm detector slits. The resolution, as determined from the low-temperature half width at half maximum (HWHM) of the $\mathbf{Q}_s$ superstructure reflection, is 0.002° HWHM (0.9×10^{-4} Å^{-1}). Figure 1(b) shows a θ scan at 104 K, in which the BC and NC components are clearly visible. In Fig. 1(b), the BC has been fitted to a $\mathcal{L}$ line shape. The NC, usually fitted to $\mathcal{L}^2$ [11,12], was found to be better fitted to a $\mathcal{L}^{1.7}$ line shape. Finally, Fig. 1(b) shows that the BC and NC are shifted by 0.02° ($\sim 10^{-3}$ Å^{-1}). This feature will be discussed later.

The peak intensity at the $\mathbf{Q}_s$ reciprocal position is displayed in Fig. 1(a). Below T_c, a fit to a $(T - T_c)^{2\beta}$ power law assuming $\beta = 0.36$, as expected for a 3D-Heisenberg order parameter, yields $T_c = 100 \pm 0.2$ K, which is consistent with previous studies [11,12]. Above T_c, the behavior of the peak intensity is mainly due to the presence of the NC, which is still visible at least 15 K above the phase transition. The temperature dependence of the BC and NC widths is indicated in Fig. 1(a), and found to be consistent with previous studies as well [11,12].

In order to gain some insight into the NC and BC spatial distribution, we have recorded x-ray diffraction patterns around $\mathbf{Q}_s$ while scanning the crystal vertical position (z) in 10 μm steps, a value which corresponds to the pinhole

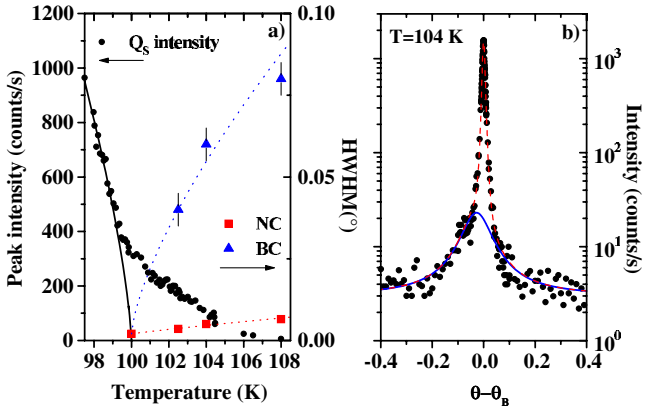

FIG. 1 (color online). (a) Temperature dependence of the peak intensity (●) of the $\mathbf{Q}_s$ superstructure reflection (20 μm $\times$ 20 μm entrance slits). The solid line is a fit to a power law. Right-hand scale, HWHM of the BC (▲) and the NC (■). The lines are guides for the eye. (b) θ scan across $\mathbf{Q}_s$ at 104 K (200 μm $\times$ 200 μm entrance slits). Intensity scale is logarithmic. The dashed line is a sum of a $\mathcal{L}$ (solid line) and $\mathcal{L}^{1.7}$ line shape (see text).

size. The graphs displayed in Fig. 2 give the patterns integrated intensity as a function of z for temperatures between 110 K and 115 K. These graphs show the presence of 20 to 100 μm regions in which the intensity is several times larger than average. We checked these results against mosaic effect by performing the same z scans at slightly different θ angles. Consistently with these results, increasing the beam size (pinhole) to 100 μm made the curves much smoother.

The 2D patterns obtained from the CCD camera clearly explain the origin of these strong variations: the BC is observed for every beam position on the sample [Fig. 3(a) and 3(c)], while the NC dominates the scattering

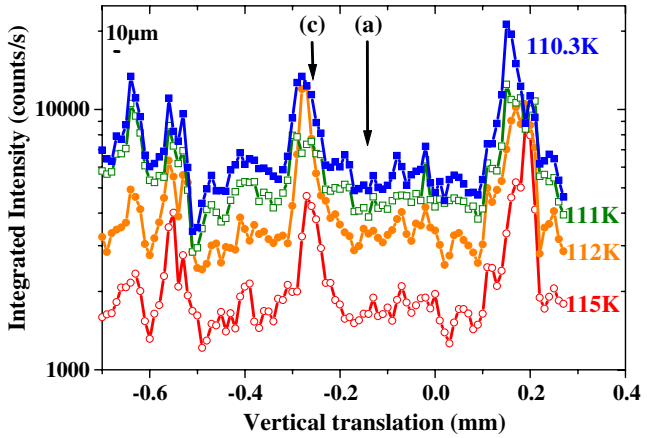

FIG. 2 (color online). Integrated intensity around the $\mathbf{Q}_s$ reciprocal position as a function of the vertical translation of the sample. Intensity scale is logarithmic. The two 2D maps obtained at the positions indicated by arrows are displayed in Fig. 3(a) and 3(c).

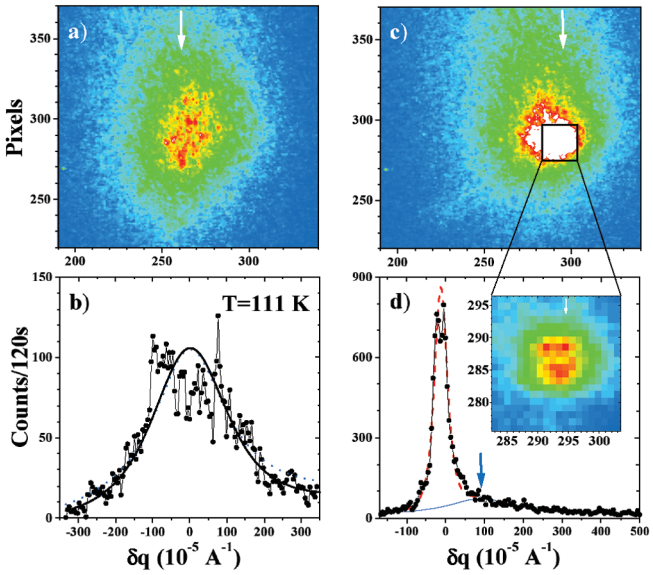

FIG. 3 (color). (a), (c) 2D patterns obtained at the $\mathbf{Q}_s$ superstructure peak intensity position for two different z positions of the beam, corresponding to the arrows in Fig. 2. The same logarithmic color scale is used for both images. Saturated values are shown in white. (b), (d) display the vertical profiles indicated by white arrows in (a), (c). In (b) the (dotted) solid lines are fits to a ($\mathcal{L}^2$) $\mathcal{L}$ line shape. In (d) the dotted line is a sum of a $\mathcal{L}^2$ and a $\mathcal{L}$ line shape (solid line) for the NC and the BC, respectively. The (blue) arrow points the BC maximum. The inset in (d) is a zoom of (c) around the NC, in linear color scale.

in the high intensity regions [Fig. 3(c)]. In a few BC dominated regions, θ scans were performed to check for the absence of NC. The maximum intensity of the BC was found to only vary within a factor 2 throughout the z scans, as shown in Fig. 2. Finally, the intensity variations shown in Fig. 2 were also observed *below* T_c, indicating that the order parameter is more developed in regions where the NC is observed above T_c.

Consistently with the θ-scan measurements, Fig. 3 shows that the maxima of the BC and the NC are not at the same position. The shift is about 10^{-3} Å^{-1} in the vertical direction. Although it was not discussed there, a similar shift is also apparent in Fig. 3 of Ref. [11]. Such an effect was also observed close to the first order antiferrodistortive transition in $RbCaF_3$ [20]. In both compounds, this shows that the NC and the BC originate from regions with different lattice parameters.

This first result gives clear evidence that an inhomogeneous distribution of the NC is observed in the sample, and that it is not the case for the BC. Incidentally, this demonstrates that the NC and the BC can be disentangled by microdiffraction, which illustrates the potential value of this technique to test phase transitions theories.

The second important result of this study is obtained using the coherence properties of our x-ray beam: the 2D patterns obtained around $\mathbf{Q}_s$ display static speckles on *both* the BC and NC, as shown in Fig. 3 at $T = 111$ K. This type of speckle patterns was observed in all regions of the sample we have studied. The HWHM of the sharpest speckles is about $\Delta q \sim 8 \times 10^{-5}$ Å^{-1}, which gives a direct space distance of $2\pi/\Delta q \sim 8$ μm. This shows that the speckles width is dominated by the pinhole size [21]. In Fig. 3, the patterns have been obtained with 2 mn exposure time. During a longer exposure time of 20 mn, no sizeable evolution of the pattern was observed.

The implications of this observation are different for each of the two components. Concerning the NC, the few speckles observed [see inset in Fig. 3(d)] are due to the diffraction of a disordered set of quasistatic domains of the low-temperature phase. The average size of these domains is given by the HWHM of the NC envelope curve, which amounts to 2 μm at $T_c + 11$ K.

Different models have been proposed to explain the occurrence of the NC close to phase transitions. Some are based on the presence of quenched defects, while others consider the phenomenon to be an intrinsic effect [9]. In both cases, however, strain fields are thought to be at the origin of the NC. Considering the absence of NC in large zones of the crystal, it seems very unlikely for the NC to result from an intrinsic effect.

In order to explain the universal character of the NC phenomenon, mechanisms based on long-range strains have been proposed [23], following Ref. [24]. These models rely on the presence of random bonds and/or a small density of impurities, which make T_c dependent on position $\mathbf{r}$ through a local compression or expansion of the lattice. Conditions on the $T_c(\mathbf{r})$ correlation function make the transition belong to a "super-universality-class," with critical exponents close to the experimental values. Long-range strains are believed to be due to dislocation dipoles, at least in Ho (Ref. [10]) and Tb (Ref. [25]).

Our observations of an inhomogeneous set of quasistatic domains makes the hypothesis of a nucleation of the low-temperature phase around defects, such as dislocations dipoles, very plausible. This is consistent with the NC position being shifted with respect to the BC one [20]. In this respect, it is noteworthy that the 20 to 100 μm regions of existence of the NC are similar in size to the skin thickness reported in Ref. [12]. However, the definitive proof that the NC occurs around dislocations is still missing. Such evidence could have been obtained from a concomitant study of the main Bragg reflections, but the experimental setup did not enable us to keep the same 10 μm $\times$ 10 μm zone illuminated during θ rotations.

The other important observation is the presence of static speckles in the BC patterns at all studied temperatures. In previous studies [16], the BC x-ray scattering has been shown to be due to the sum of the soft mode and the CP contribution. Soft modes frequencies being far beyond the frequencies accessible by x-ray intensity fluctuation spectroscopy, they contribute to a smooth broad scattering

without any speckles [21]. Moreover, since close to T_c, the CP q dependence has the same HWHM as the x-ray BC within 10% [16], we suggest that the presence of speckles in the BC scattering is related to the neutron CP.

As in the case of the NC, two types of theories have attempted to account for the CP, either through *intrinsic* anharmonic effects or through a linear coupling of the soft mode to static (*frozen*) or slowly relaxing defects of appropriate symmetry [7]. The main objection against intrinsic scenarios has always been that a characteristic time scale in the MHz range [5] seems difficult to generate, starting from phonon frequencies in the THz or GHz range. The observation of very long-lived speckles on the BC only reinforces this argument. Concerning length scales, we find that the BC appears to be homogeneous on a 10 μm scale, which implies that the defects involved in the CP are of a different nature than those which induce the NC. From neutron data, an estimation of the concentration c of CP-active impurities per unit cell [7] gives $c = 1.2 \times 10^{-5}$. This corresponds to one impurity every 5000 nm^3, a volume far smaller than our 10 μm beam resolution. Moreover, the static character of the BC speckles favors the model of *frozen cell defects* linearly coupled to the order parameter [7,26]. However, it does not rule out the additional presence of relaxing cell defects, whose contribution to the speckle patterns would be smoothed out by time averaging.

This study shows that CXD is a powerful tool in order to gain insight into unresolved issues near phase transitions, such as the neutron CP and the x-ray NC. By coupling a microbeam probe with a coherent beam, we demonstrate it is possible to disentangle the NC and the BC of the critical scattering, and to give evidence for the quasistatic character of both phenomena. These results are in favor of surface long-range order defects to explain the NC, and of frozen impurities to explain the CP.

We thank A. Moussaïd, A. Madsen, and G. Baldinozzi for help during the ID10a experiments, T. Metzger for help during preliminary experiments at ID01, and B. Hehlen and E. Courtens for kindly providing us with the $SrTiO_3$ single crystal. We are indebted to F. Livet and F. Picca for the coherent diffraction setup and the data analysis.

[1] R. A. Cowley, Adv. Phys. **29**, 1 (1980); A. D. Bruce, Adv. Phys. **29**, 111 (1980); A. D. Bruce and R. A. Cowley, Adv. Phys. **29**, 219 (1980).
[2] T. Riste, E. Samuelsen, K. Otnes, and J. Feder, Solid State Commun. **9**, 1455 (1971).
[3] S. Shapiro, J. D. Axe, G. Shirane, and T. Riste, Phys. Rev. B **6**, 4332 (1972).
[4] J. Töpler, B. Alefeld, and A. Heidemann, J. Phys. C **10**, 635 (1977).
[5] G. F. Reiter, W. Berlinger, K. A. Müller, and P. Heller, Phys. Rev. B **21**, 1 (1980).
[6] J. B. Hastings, S. M. Shapiro, and B. C. Frazer, Phys. Rev. Lett. **40**, 237 (1978).
[7] B. I. Halperin and C. M. Varma, Phys. Rev. B **14**, 4030 (1976).
[8] S. Andrews, J. Phys. C **19**, 3721 (1986).
[9] R. A. Cowley, Phys. Scr. **T66**, 24 (1996).
[10] T. R. Thurston, G. Helgesen, J. P. Hill, D. Gibbs, B. D. Gaulin, and P. J. Simpson, Phys. Rev. B **49**, 15 730 (1994).
[11] K. Hirota, J. P. Hill, S. M. Shapiro, G. Shirane, and Y. Fujii, Phys. Rev. B **52**, 13 195 (1995).
[12] H. Hünnefeld, T. Niemöller, J. R. Schneider, U. Rütt, S. Rodewald, J. Fleig, and G. Shirane, Phys. Rev. B **66**, 014113 (2002).
[13] G. M. Watson, B. D. Gaulin, Doon Gibbs, T. R. Thurston, P. J. Simpson, S. M. Shapiro, G. H. Lander, Hj. Matzke, S. Wang, and M. Dudley, Phys. Rev. B **53**, 686 (1996).
[14] R. Wang, Y. Zhu, and S. M. Shapiro, Phys. Rev. Lett. **80**, 2370 (1998).
[15] A. Gibaud, H. You, S. M. Shapiro, and J. Y. Gesland, Phys. Rev. B **42**, 8255 (1990).
[16] G. Shirane, R. A. Cowley, M. Matsuda, and S. M. Shapiro, Phys. Rev. B **48**, 15 595 (1993).
[17] M. Sutton, S. G. J. Mochrie, T. Greytak, S. E. Nagler, L. E. Berman, G. A. Held, and G. B. Stephenson, Nature (London) **352**, 608 (1991).
[18] K. Ludwig, F. Livet, F. Bley, J.-P. Simon, R. Caudron, D. Le Bolloch, and A. Moussaid, Phys. Rev. B **72**, 144201 (2005).
[19] D. Le Bolloch, F. Livet, F. Bley, T. Schulli, M. Veron, and T. H. Metzger, J. Synchrotron Radiat. **9**, 258 (2002).
[20] T. W. Ryan, R. J. Nelmes, R. A. Cowley, and A. Gibaud, Phys. Rev. Lett. **56**, 2704 (1986).
[21] The degree of coherence of the speckle pattern shown in Fig. 3(a) is $\beta \sim 3\%$. This low value is mainly due to the large maximum path length difference $\Delta \sim 2\mu^{-1}\sin^2\theta$ ($\sim$3.6 μm) compared to the longitudinal coherence length ($\sim$1.4 μm) given by the monochromator [22]. Note that the smooth soft mode contribution to the BC decreases β as well.
[22] D. Le Bolloc'h, S. Ravy, J. Dumas, J. Marcus, F. Livet, C. Detlefs, F. Yakhou, and L. Paolasini, Phys. Rev. Lett. **95**, 116401 (2005).
[23] M. Altarelli, M. D. Núñez-Regueiro, and M. Papoular, Phys. Rev. Lett. **74**, 3840 (1995); M. Papoular, M. D. Núñez-Regueiro, and M. Altarelli, Phys. Rev. B **56**, 166 (1997).
[24] A. Weinrib and B. I. Halperin, Phys. Rev. B **27**, 413 (1983).
[25] P. M. Gehring, K. Hirota, C. F. Majkrzak, and G. Shirane, Phys. Rev. Lett. **71**, 1087 (1993).
[26] Such a random-field behavior is known to add a $\mathcal{L}^2$ contribution to the scattering above T_c. As shown in Fig. 3(b), the BC is too speckled to distinguish between a $\mathcal{L}^2$ and a $\mathcal{L}$ line shape.